International Journal of Microwave and Wireless Technologies

cambridge.org/mrf

Complementary Sierpinski Knopp fractal antenna for emergency management system

Paulkani Iyampalam and Indumathi Ganesan

Department of Electronics and Communication Engineering, Mepco Schlenk Engineering College, Sivakasi-626005, Tamil Nadu, India

Research Paper

Cite this article: Iyampalam P, Ganesan I (2020). Complementary Sierpinski Knopp fractal antenna for emergency management system. *International Journal of Microwave and Wireless Technologies* **12**, 1029–1038. https://doi.org/10.1017/S1759078720000343

Received: 25 June 2019
Revised: 19 March 2020
Accepted: 20 March 2020
First published online: 16 April 2020

Keywords:
Emergency management system; fractal antenna; Public Protection and Disaster Relief (PPDR) communication; Sierpinski Knopp curve

Author for correspondence:
Paulkani Iyampalam, E-mail: paulkani64@gmail.com

Abstract

In this paper, the design and analysis of a complementary Sierpinski Knopp fractal antenna are presented. It is realized by applying the Sierpinski Knopp space-filling curve on the basic square monopole antenna. The performance metrics of the antenna such as S_{11} (reflection coefficient), voltage standing wave ratio, radiation pattern, gain and current distribution at resonant frequencies are analyzed by using ANSYS Electronic Desktop software package. FR4 dielectric material is used as a substrate in which the radiating element of an antenna is printed. Vector network analyzer and anechoic chamber are used for measuring the fabricated antenna in order to validate the simulated data. The proposed antenna resonates at three frequencies that are 2.08, 4.93, and 6.46 GHz with a reflection coefficient of −20.5, −23.1, and −24.3 dB, respectively. The suggested antenna covers the frequency bands for mobile satellite service, Public Protection and Disaster Relief communication devoted to the emergency management system and INSAT C band applications.

Introduction

In recent years, there has been a rise in natural disasters as well as man-made disasters such as cyclones, earthquakes, tsunami floods, terrorist attacks, and accidents. To rescue people from such disasters, Public Protection and Disaster Relief (PPDR) communication network was developed and organized by the government and agencies [1]. Federal communications commission allocated frequency range from 4.94 to 4.99 GHz for public safety band. Satellite communication also plays a significant role in emergency conditions. The voice and data communications are made by utilizing the satellites. Mobile satellite service (MSS) and Indian National Satellite System or INSAT are some of the services operated for rescue operations. INSAT is a geostationary satellite launched by ISRO that is used for many purposes, but the important usage is a search and rescue operation. Reliable communication infrastructure is the major part of an emergency system, which allows the operator to rescue the people by collecting the data from the monitoring devices in the disaster area [2].

Reliable communication requires an antenna with small size, lightweight, ease of fabrication, and supports multiband operation. Patch antennas are suitable for achieving the said requirements [3], while the disadvantage is it does not support multiband. Nowadays, wireless communication devices such as laptops, tablet, and smartphones should be able to support multiple applications with compact size. A large number of works has been reported for realizing a compact antenna with multiband operation using several techniques including applying different fractal geometries to the antenna [4], employing various feeding techniques [5, 6], utilizing self-complementary structure [7], and using substrate integrated waveguide (SIW) [8]. Among these techniques, a fractal is one of the most popular techniques due to its properties of self-similarity and space-filling which provide multiband behavior and small size.

In recent days, several antennas are developed based on the fractalizing techniques which include Koch snowflake fractal [9], Sierpinski fractal [10–12], periwinkle flower-shaped fractal [13], "X" shaped fractal [14], Minkowski curve [15, 16], and spidron fractal [17] for various wireless applications. However, to the best of the authors' knowledge, a limited number of antennas is reported by the researcher for emergency management. A capacitive feed stepped T-shape patch antenna is designed for US public safety band and long term evolution [18]. The dimension of the stated antenna is 193.75×168.75 mm^2.

The antenna in [19] operated in quad-band with a size of 160×178 mm^2. These antennas are larger in size. Therefore, fractal geometry is utilized to attain a compact size [20–22]. The design of a multiband antenna based on the perturbed Sierpinski geometry is reported in [20]. In addition to that, the particle swarm optimization technique is carried out for synthesizing antenna parameters. Fibonacci word fractal antenna with two rectangular slots is stated in [21] for public safety applications. Whale optimization is implemented for enhancing efficiency. An "I" shaped fractal antenna is designed by subtracting two parallel edges from the center of the

CAMBRIDGE UNIVERSITY PRESS

rectangular patch. It is inspired by the Sierpinski carpet structure [22]. The previously developed antenna's structure is complicated to design and larger.

In this paper, design, simulation, and analysis of a complementary Sierpinski Knopp (CSK) fractal antenna are reported for MSS, PPDR, and INSAT C band communication. In the section "Numerical formulation", the numerical formulation and generation of the Sierpinski Knopp curve for CSK antenna are described. The section "Antenna design methodology" expresses the antenna design methodology and parametric analysis of the design variables. The discussion of the simulated and measured results is elaborated in the section "Measured results and discussion" and finally, the work is concluded in the last section.

Numerical formulation

The monopole antenna is widely used as the most popular antenna due to its small size and ease of fabrication. In this work, a square monopole antenna is taken as the basic design for constructing the projected fractal antenna. The parameters of the monopole antenna can be determined by using the following formula [3]

$$W = \frac{c}{2 \times f_r \times \sqrt{\xi_r + 1/2}}, \tag{1}$$

$$\xi_{eff} = \frac{\xi_r + 1}{2} + \frac{\xi_r - 1}{2}\left[1 + \frac{12h}{W}\right]^{-1/2}, \tag{2}$$

$$L = \frac{c}{2 \times f_r \times \sqrt{\xi_{eff}}} - 2\Delta L, \tag{3}$$

$$\Delta L = h \times 0.412\left[\frac{(\xi_{eff} + 0.3)((W/h) + 0.264)}{(\xi_{eff} - 0.258)((W/h) + 0.8)}\right]. \tag{4}$$

Here, W and L are the width and length of the patch, c is the velocity of light ($c = 3 \times 10^8$ m/s), f_r is the resonance frequency, ξ_r is the dielectric constant, h is the thickness of the substrate, and ΔL is the incremental length due to the fringing.

Iterated Function System (IFS)

The IFS is a mathematical method to generate the fractal structure by describing scaling, rotation, and transformation of the kernel structure. It uses the set of self-affine transformations for fractal geometry generation. The IFS matrix of the proposed CSK fractal can be expressed as [23]

$$P(x'\ y') = \begin{pmatrix} a & b \\ c & d \end{pmatrix}\begin{pmatrix} x' \\ y' \end{pmatrix} + \begin{pmatrix} e \\ f \end{pmatrix}, \tag{5}$$

$$P_1(x'\ y') = \frac{1}{2}\begin{pmatrix} 1 & 0 \\ 0 & 1 \end{pmatrix}\begin{pmatrix} x' \\ y' \end{pmatrix} + \frac{1}{2}\begin{pmatrix} 0 \\ 0 \end{pmatrix}, \tag{6}$$

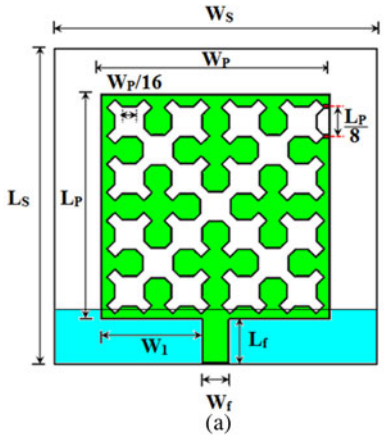

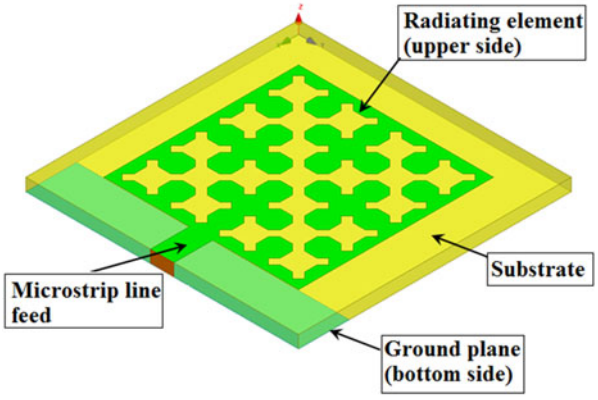

Fig. 1. Geometry of the proposed CSK fractal antenna. (a) Front view, (b) 3D view.

Table 1. Dimensions of the CSK antenna

Design variables	Value (mm)	Design variables	Value (mm)
L_s	35	W_s	35
L_p	25	W_p	25
L_g	6.5	W_g	35
L_f	5	W_f	3
W_1	11	h	1.6

$$P_2(x'\ y') = \frac{1}{2}\begin{pmatrix} 0 & -1 \\ 1 & 0 \end{pmatrix}\begin{pmatrix} x' \\ y' \end{pmatrix} + \frac{1}{2}\begin{pmatrix} 2 \\ 0 \end{pmatrix}, \tag{7}$$

$$P_3(x'\ y') = \frac{1}{2}\begin{pmatrix} 0 & 1 \\ -1 & 0 \end{pmatrix}\begin{pmatrix} x' \\ y' \end{pmatrix} + \frac{1}{2}\begin{pmatrix} 2 \\ 2 \end{pmatrix}, \tag{8}$$

$$P_4(x'\ y') = \frac{1}{2}\begin{pmatrix} 1 & 0 \\ 0 & 1 \end{pmatrix}\begin{pmatrix} x' \\ y' \end{pmatrix} + \frac{1}{2}\begin{pmatrix} 2 \\ 0 \end{pmatrix}. \tag{9}$$

Let us assume that $P_1, P_2, \ldots, P_n$ are the series of linear self-affine transformations and S be the initial structure. The final geometry

https://doi.org/10.1017/S1759078720000343 Published online by Cambridge University Press

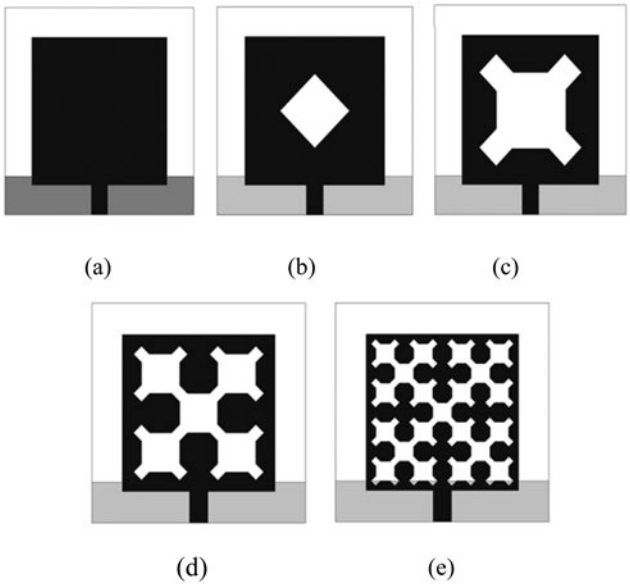

Fig. 2. Iteration Stages of fractal antenna. (a) Basic design, (b) 0th iteration, (c) 1st iteration, (d) 2nd iteration, (e) 3rd iteration.

is obtained by uniting all four transformations. It can be expressed as

$$P(S) = \sum_{n=1}^{N} P_n(S). \tag{10}$$

The higher-order iterations of the fractal are achieved by repeating this process. The IFS is also referred to as a multiple reduction copy machine. The fractal similarity dimension (D) can be calculated as [21]

$$D = \frac{\log n}{\log[1/f]}, \tag{11}$$

where n is the number of copies and f is the scaling factor. In the case of the Sierpinski Knopp curve, $n = 4$ and $f = 1/2$. The fractal dimension is 2 for the proposed CSK antenna.

Antenna design methodology

Antenna configuration

The projected CSK fractal antenna is assembled on the FR4 dielectric material with a volume of $35 \times 35 \times 1.6\ \text{mm}^3$. Figures 1(a) and 1(b) show the front and 3D view of the proposed CSK fractal antenna. The novelty of the proposed antenna lies in the antenna radiating structure. Also, a slot-loading technique is employed in order to increase the number of operating bands. The structure consists of the Sierpinski Knopp curve inspired square monopole antenna on the upper side of the substrate and partial ground plane on the flipside.

The microstrip feed line is bonded to the female SMA connector having 50Ω impedance for electrifying the antenna. The motivation of such fractal geometry is to increase the electrical length and bandwidth of the antenna. The variables are assigned to each element of the antenna for parametric analysis as follows: L_s – length of the substrate, W_s – width of the substrate, h – thickness of the substrate, L_p – length of the microstrip patch, W_p – width of the microstrip patch, L_g – Length of the ground plane, W_g – width of the ground plane, L_f – length of the microstrip feed line, and W_f – width of the microstrip feed line. The distance between the feed line and edge of the patch is denoted by W_1.

To achieve the desired results, the dimensions of the substrate material, ground plane, microstrip patch, and feed line have been optimized by performing the parametric analysis. The performance metric of the antenna is investigated by utilizing the ANSYS HFSS. The values of the design variables are listed in Table 1, which yields the optimum results. The square of dimension $25 \times 25\ \text{mm}^2$ has been chosen as a kernel to create the geometry of the projected fractal antenna. Initially, the square patch is fragmented into two isosceles triangles. The various iteration stages in the development of the proposed CSK fractal antenna from the basic design to 3^{rd} iteration is depicted in Fig. 2.

Figure 2(a) shows the square monopole antenna which is modified in such a way to achieve the desired frequency bands by using fractal geometry. As seen in Fig. 2(b), a square with an area of $8.83 \times 8.83\ \text{mm}^2$ has been placed in the middle and rotated by 90°. The resulted diamond-shaped patch is etched from the basic square monopole, which is named as 0^{th} iteration. For the first iteration, the square monopole is sliced into four smaller squares. The diamond-shaped patch is scaled down by 2 and

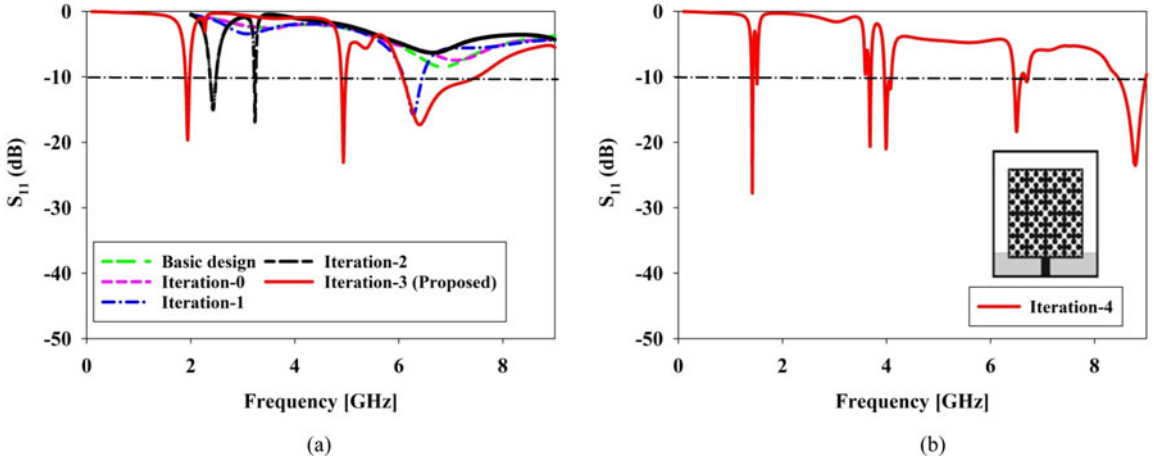

Fig. 3. Effect on S_{11} at different iteration levels. (a) Basic design, Iteration-0, Iteration-1, Iteration-2 and Iteration-3, (b) Iteration-4.

https://doi.org/10.1017/S1759078720000343 Published online by Cambridge University Press

Table 2. Comparative characteristics of antenna at various iterations

Antenna iteration	Resonant frequencies [GHz]	S_{11} [dB]	Bandwidth [MHz]	Frequency range [GHz]	VSWR	Gain [dBi]
Basic design	6.8	−8.5	–	–	2.2	4
0th iteration	7.1	−7.46	–	–	2.46	4.1
1st iteration	6.28	−15.74	370	6.06–6.46	1.39	3.4
2nd iteration	2.43	−14.97	120	2.37–2.49	1.43	1.96
	3.23	−16.88	30	3.22–3.25	1.33	3.8
Proposed antenna (3rd iteration)	1.94	−19.6	80	1.90–1.98	1.24	3.62
	4.95	−24	80	4.91–4.99	1.2	3
	6.41	−17.3	1400	6.07–7.51	1.31	3.76
4th iteration	1.42	−24.98	10	1.41–1.43	1.13	4.5
	3.68	−20.63	40	3.66–3.7	1.21	−3.6
	3.99	−21.03	40	3.96–4.0	1.19	−0.74
	6.5	−18.34	140	6.45–6.59	1.27	0.43
	8.79	−23.46	500	8.9–8.4	1.14	9

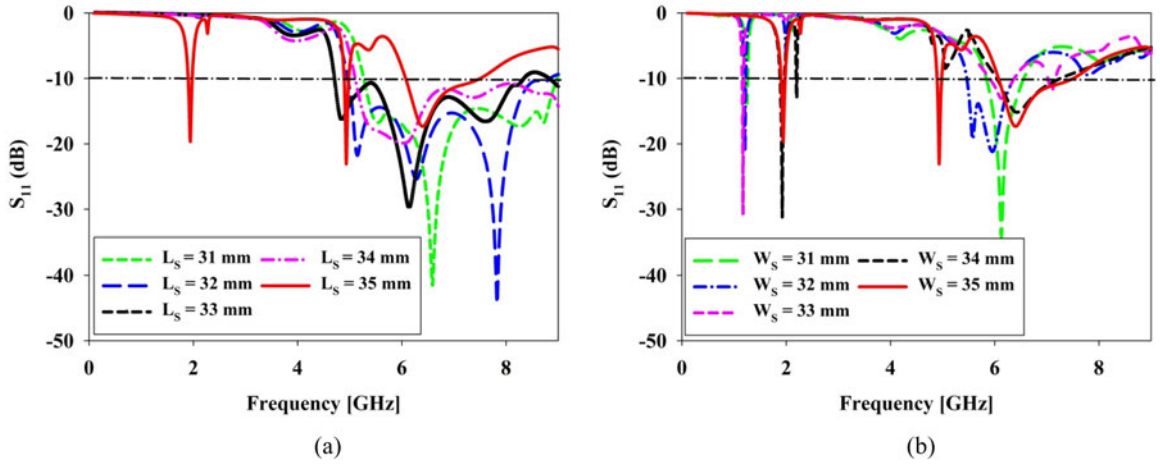

Fig. 4. Effect on S_{11} with variation of (a) length of the substrate L_S, (b) width of the substrate W_S.

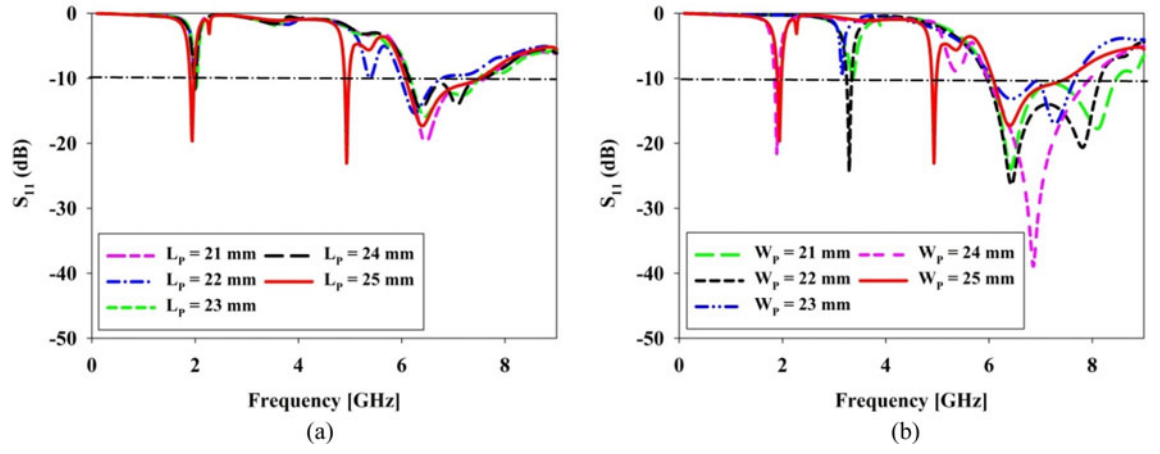

Fig. 5. Effect on S_{11} with variation of (a) length of the patch L_P, (b) width of the patch W_P.

https://doi.org/10.1017/S1759078720000343 Published online by Cambridge University Press

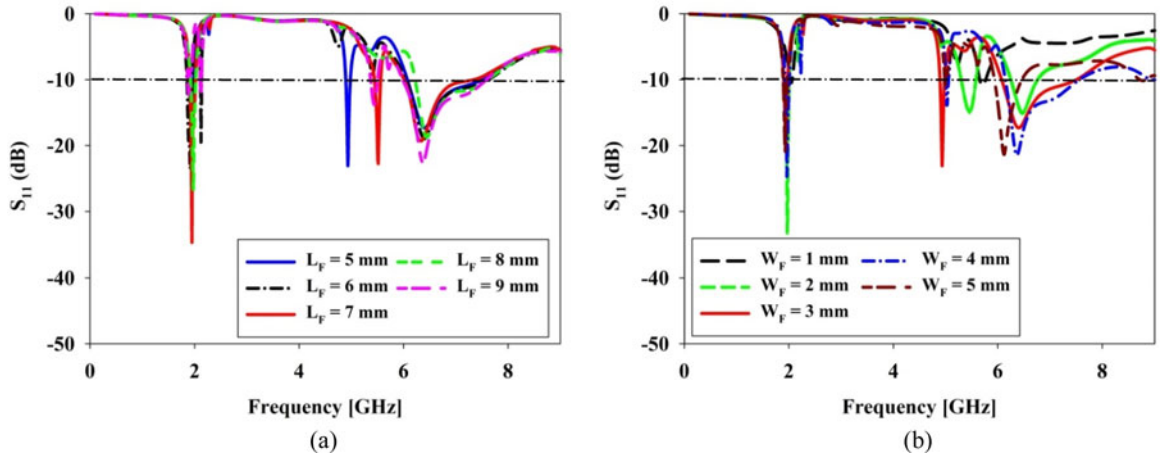

Fig. 6. Effect on S_{11} with variation of (a) length of the feed line L_F, (b) width of the feed line W_F.

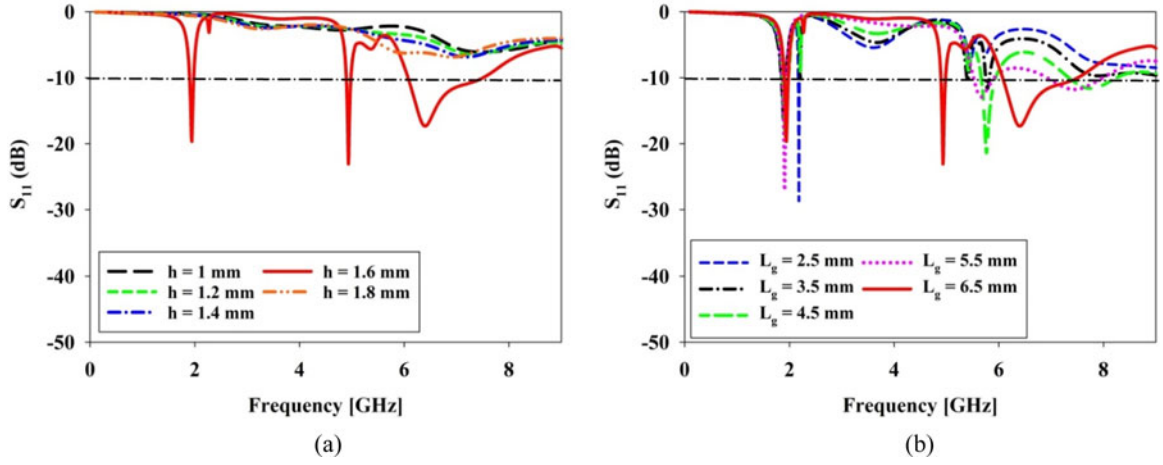

Fig. 7. Effect on S_{11} with variation of (a) substrate thickness h, (b) length of the ground plane L_g.

located in the middle of each four squares. The edges of all diamond-shaped patches are joined and removed from the kernel. Antenna design at the end of the first iteration is displayed in Fig. 2(c). This recursive process is repeated for obtaining the second and third iterations of the fractal antenna that are depicted in Figs 2(d) and 2(e), respectively.

Parametric study

The parametric analysis of the fractal antenna has been carried out for achieving better performance. In this study, the size of the substrate, ground plane, feed line, and square patch is considered for the parametric analysis. The S_{11} at different iteration levels from basic design to iteration-4 of the fractal antenna is shown in Figs 3(a) and 3(b). The antennas in the basic design and 0^{th} iteration have not an effective S_{11}, which is higher than −10 dB. In the first iteration, antenna resonates at 6.28 GHz with −15.8 dB reflection coefficient.

The dual resonance appears at the second iteration where the S_{11} values are −15.02 dB at 2.42 GHz and −16.88 dB at 3.23 GHz. The required triple band with improved S_{11} and bandwidth is achieved by the suggested fractal antenna in the 3rd iteration. Reflection coefficients are reduced to −19.6, −24, and −17.3 dB at the corresponding resonant frequencies of 1.94, 4.95, and 6.41 GHz, respectively.

Table 2 presents the comparative characteristics of the antenna at various iterations. It is noted that the number of resonant frequency increases as the number of iterations increases because of the fractal structure.

The bandwidth and gain of the antenna are decreased at some frequency bands and voltage standing wave ratio (VSWR) is acceptable (VSWR≤2) by increasing the iteration. When doing it up to the 3rd iteration, the performance such as bandwidth and gain is found to be better than the results obtained during 4th iteration. On the other hand, it is observed that moving from 3rd iteration to 4th iteration, the operating frequency is deviating and the antenna becomes quite complicated and its fabrication becomes difficult. Therefore, the number of iteration in the proposed work is limited to 3rd iteration.

The geometrical parameters such as L_S, W_S, L_P, W_P, L_g, L_F, W_F, and h are varied individually while the other parameters are remaining constant. The length (L_S) and width (W_S) of the

https://doi.org/10.1017/S1759078720000343 Published online by Cambridge University Press

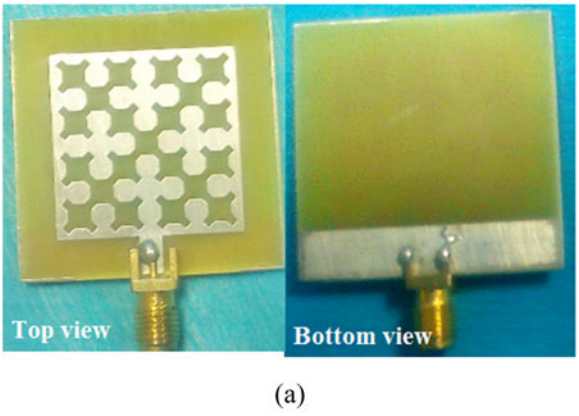

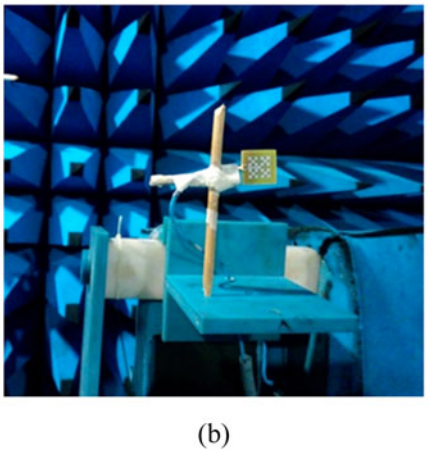

Fig. 8. (a) Fabricated CSK fractal antenna, (b) measurement setup in the anechoic chamber.

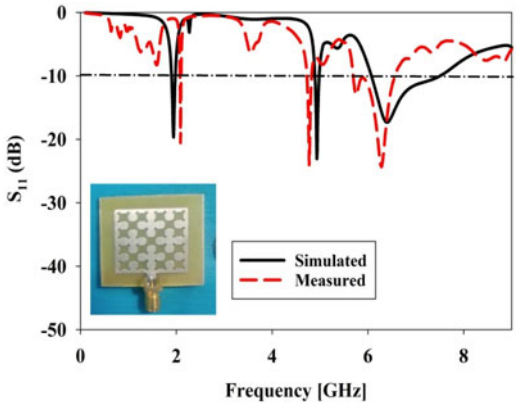

Fig. 9. Simulated and measured S_{11}.

substrate are changed from 31 to 35 mm. The slight change in the substrate length (L_S) alters the resonance behavior of the antenna. The S_{11} versus frequency for different L_S and Ws is shown in Figs 4 (a) and 4(b), respectively. The required triple-band resonance characteristics with better performance are observed at $L_S = W_S = 35$ mm. From Fig. 4(b), it can be found that the frequency is shifted from 6 to 4.95 GHz due to changes in the substrate width (W_S).

The patch length L_P and width W_P are varied from 21to 25 mm with a step of 1 mm. The impedance matching is found well at $L_P = 25$ mm.

As seen in Fig. 5(a), the antenna resonates at the higher frequencies above 6 GHz for the values of L_P from 21 to 24 mm. The antenna has dual-band operation for the values of W_P

Table 3. Comparison of simulated and measured data of projected CSK fractal antenna

Results obtained	Resonant frequency [GHz]	S_{11} [dB]	Bandwidth [MHz]	Bandwidth [%]	Frequency range [GHz]	VSWR
In simulation	1.94	−19.6	80	4.1	1.90–1.98	1.24
	4.95	−24	80	1.6	4.91–4.99	1.2
	6.41	−17.3	1400	21.6	6.07–7.51	1.31
In measurement	2.08	−20.5	30	1.4	2.07–2.10	1.21
	4.93	−23.1	110	2.2	4.90–5.01	1.25
	6.46	−24.3	870	13.4	5.87–6.74	1.14

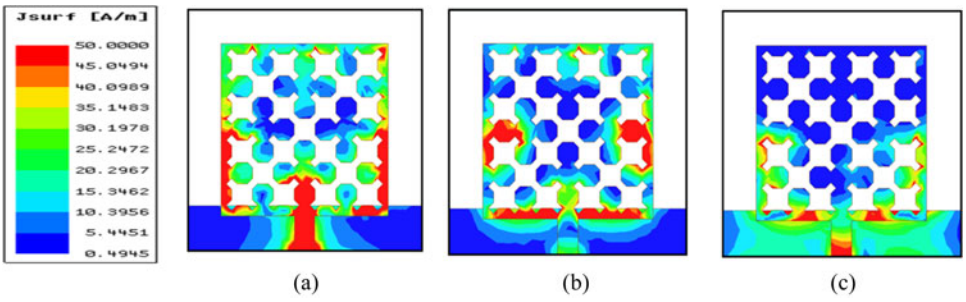

Fig. 10. Current distribution at (a) 2.08 GHz, (b) 4.93 GHz, and (c) 6.46 GHz.

https://doi.org/10.1017/S1759078720000343 Published online by Cambridge University Press

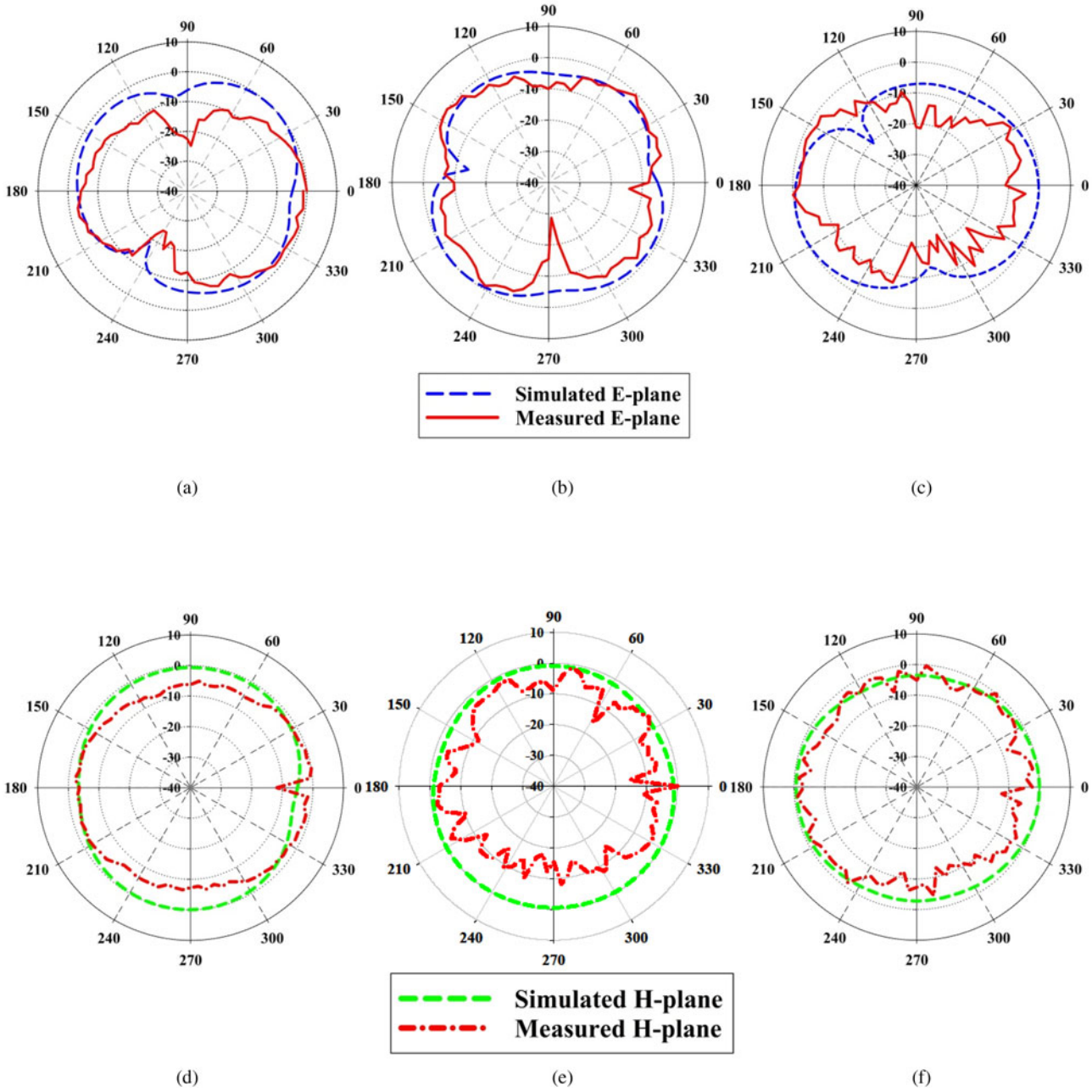

Fig. 11. Simulated and measured radiation pattern in *E*-plane at (a) 2.08 GHz, (b) 4.93 GHz, and (c) 6.46 GHz; *H*-plane at (d) 2.08 GHz, (e) 4.93 GHz, and (f) 6.46 GHz.

from 21 to 24 mm and triple-band operation at 25 mm which is presented in Fig. 5(b).

In a further study, the feed line length (L_F) is varied from 5 to 9 mm with an interval of 1 mm and the effect on S_{11} is depicted in Fig. 6(a). The optimum value is chosen as 5 mm because of its resonance at 4.95 GHz, which is the required band for PPDR applications. The effect on S_{11} with respect to various feed width (W_F) is presented in Fig. 6(b). The resonant frequency is shifted to the lower side as W_F increases. It is noted that the antenna has good performance at 3 mm. The substrate thickness (h) also plays an important role in the antenna design. Figure 7(a) shows the impact on the S_{11} by varying h. A poor impedance matching is perceived for the values of h ranges from 1 to 1.6 mm. Antenna impedance is well matched at 1.6 mm. Therefore, the value of 1.6 mm is selected as the thickness of the substrate (h). Figure 7(b) shows the effect on S_{11} against frequency for different ground plane length (L_g). The better result is attained at 6.5 mm.

All the geometrical parameters of the proposed CSK fractal antenna are chosen according to the parametric analysis for achieving optimum results.

Measured results and discussion

The prototype of the projected antenna is fabricated using the FR4 substrate with the dielectric constant (ϵ_r) of 4.4, thickness (h) of 1.6 mm, and loss tangent (δ) of 0.002. The photo etching technique is used for fabricating the antenna. In the fabrication

https://doi.org/10.1017/S1759078720000343 Published online by Cambridge University Press

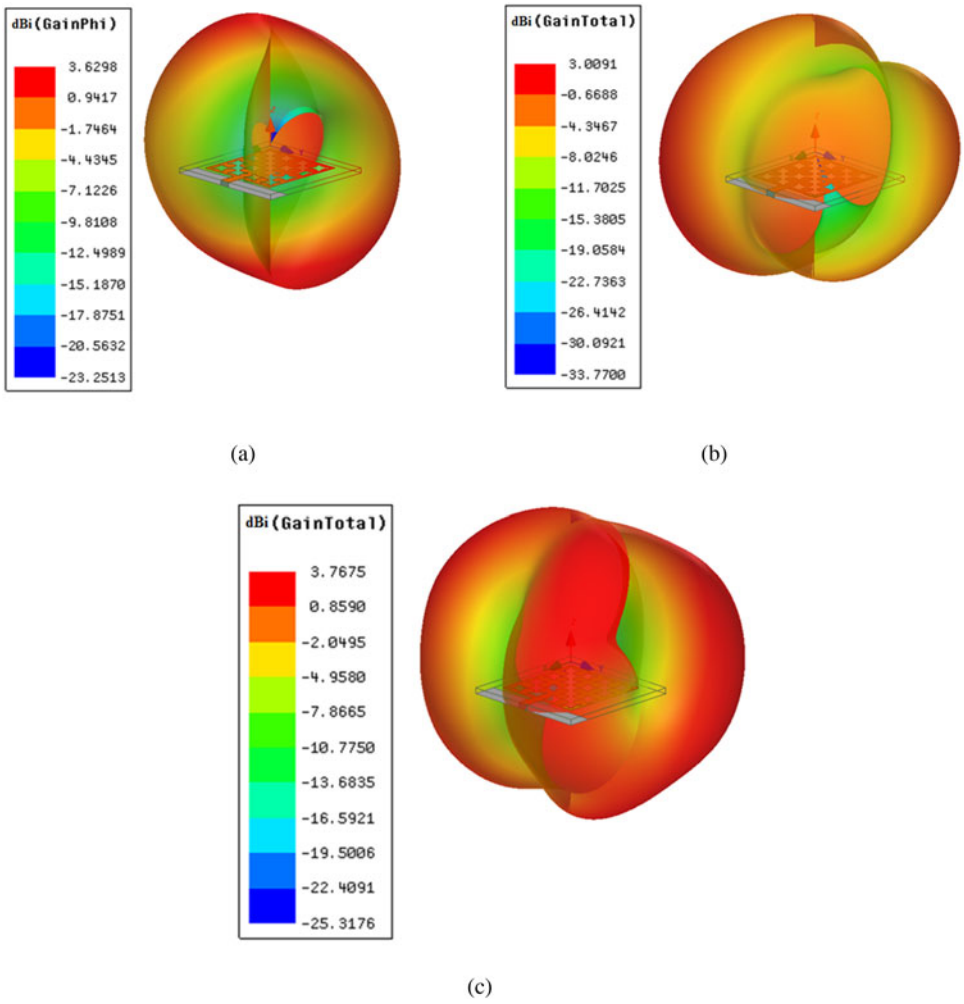

Fig. 12. 3D gain plot at (a) 2.08 GHz, (b) 4.93 GHz, and (c) 6.46 GHz.

process, the cover of the photoresist of the FR4 board is removed. Then, the transparent mask of the antenna geometry is placed over the FR4 board. The transparent mask is the image of the .dxf file, which is obtained from Ansys HFSS. Next, the FR4 board is exposed to ultra-violet (UV) light. In the final stage, the etching process is performed by placing the FR4 board in a ferric chloride solution. In order to remove unwanted photoresist material, the board is rinsed with acetone. After that, the SMA connector is soldered to the fabricated antenna.

The fabricated antenna is measured by using Agilent vector network analyzer (VNA) under an anechoic chamber in order to validate the results, which are obtained through simulation. The fabricated CSK fractal antenna and the measurement setup in the anechoic chamber are illustrated in Figs 8(a) and 8(b), respectively.

Figure 9 shows the simulated and measured S_{11} plot against frequency. It is found that the impedance bandwidths are 30 MHz (1.4% centered at 2.08 GHz), 110 MHz (2.2% centered at 4.93 GHz), and 870 MHz (13.4% centered at 6.46 GHz), respectively. Thus, the suggested CSK fractal antenna can cover the emergency management system that is PPDR (4.90–5.01 GHz), MSS (2.07–2.10 GHz), and INSAT C band (5.87–6.74 GHz) applications. The simulated and measured data of the projected CSK fractal antenna are listed in Table 3. There is a deviation between the results obtained through simulation and measurement because of the losses occurred during the fabrication and soldering of the SMA connector to the antenna.

The distributions of the current on the fractal antenna at resonant frequencies are depicted in Fig. 10. The high current density implies the high coupling while the low current density indicates less coupling. The maximum current density is distributed near the feed line and the edges of the patch at 2.08 GHz that is shown in Fig. 10(a). As seen in Fig. 10(b), the current density is highly concentrated on the lower side, left, and right side of the patch at 4.93 GHz. The coupling is high at 6.46 GHz where the maximum current is found on the ground plane as well as the lower half of the patch that is presented in Fig. 10(c).

The radiation pattern is obtained by rotating the antenna angle (θ) from 0° to 360°. For the corresponding operating frequencies, the simulated and measured *E*-plane radiation pattern is shown in Figs 11(a)–11(c). It is observed that the antenna exhibits a doughnut-shaped pattern in *E*-plane.

Figures 11(d)–11(f) show the *H*-plane radiation pattern obtained through simulation and measurement, which reveals that the antenna has an omnidirectional radiation pattern across the corresponding operating bands.

Gain is one of the important factors in the design of an antenna. It provides the maximum energy radiation in a

https://doi.org/10.1017/S1759078720000343 Published online by Cambridge University Press

Table 4. Comparison of the projected fractal antenna with the earlier antennas in the literature.

References	Antenna geometry	Resonant frequency [GHz]	Maximum bandwidth	Size (mm^2)	Gain [dBi]	Operating bands
[11]	Complementary Sierpinski gasket	3.5/5.8	150 MHz	25 × 35	5/4	Dual band
[15]	Minkowski curve	10	270 MHz	6.16 × 4.65	3.23	Single band
[16]	Minkowski curve	2.78/4.29	60.8 MHz	25.7 × 19.7	4.45/5.4	Dual band
[17]	Spidron fractal	12/13.8	1004 MHz	50 × 50	3.73/3.83	Dual band
[18]	Stepped T-shape patch	[a]	435 MHz	193.75 × 168.75	2	Single band
[19]	Patch antenna	220/470/800/4960	3/4/21/17%	160 × 178	[a]	Quad band
[20]	Perturbed Sierpinski fractal	2.55/4.96	600 MHz	23.5 × 15.5	[a]	Dual-band
[21]	Fibonacci word fractal	4.9/5.9	1000 MHz	50 × 44	2.3/4.7	Dual band
Proposed antenna	Sierpinski Knopp curve	2.08/4.93/6.46	870 MHz	35 × 35	3.62/3/3.76	Tri-band

[a]Not available.

particular direction. The 3D gain plot at 2.08, 4.93, and 6.46 GHz is depicted in Figs 12(a)–12(c), respectively. The projected CSK fractal antenna has a gain of 3.62 dBi at 2.08 GHz, 3 dBi at 4.95 GHz, and 3.76 dBi at 6.46 GHz. The comparison of the CSK fractal antenna with the existing fractal antenna is summarized in Table 4. It is noted from Table 4 that the proposed antenna is compact size in comparison with the antennas reported in [17, 18, 19, 21].

The antennas stated in [11, 15, 16, 20] have compact size but the bandwidth of those antennas is less than the proposed CSK fractal antenna. In [19], an antenna has four resonant frequencies, which is higher than the proposed antenna but the size is larger and gain is not reported. The projected CSK antenna exhibits triple-band whereas the other antennas have single and dual bands. Based on the above discussion, it can be seen that the proposed antenna is novel and useful for wireless applications include MSS, INSAT C band, and public safety band.

Conclusion

A triple-band CSK fractal antenna is proposed for wireless applications dedicated to the emergency management system, MSS, and INSAT C band applications. The prototype of the CSK is fabricated and tested. It is observed from the measurement results that the antenna has three operating frequencies of 2.08, 4.93, and 6.46 GHz with a small size $35 \times 35 \times 1.6\ mm^3$. Doughnut-shaped and omnidirectional radiation patterns are obtained in *E*- and *H*-plane. The measured results are in good accordance with the simulation results. Maximum bandwidth and gain of 870 MHz and 3.76 dBi have been observed at 6.46 GHz.

Acknowledgement. The authors wish to thank the Mepco-Agilent R&D Centre of Excellence in RF Circuit and Antenna Design, Mepco Schlenk Engineering College, Sivakasi for the support in carrying out this research work.

References

1. **Doumi TL** (2006) Spectrum considerations for public safety in the United States. *IEEE Communications Magazine* **44**, 30–37.
2. **Chiti F, Fantacci R, Maccari L, Marabissi D and Tarchi D** (2008) A broadband wireless communications system for emergency management. *IEEE Wireless Communications* **15**, 8–14.
3. **Balanis CA** (2005) *Antenna Theory: Analysis and Design*, 3rd Edn. Hoboken, New Jersey: John Wiley & Sons.
4. **Ganesan I and Iyampalam P** (2018) A review of ultra- wideband fractal antennas. IEEE International *Conference on Inventive Communication and Computational Technologies (ICICCT), Coimbatore*, pp. 1408–1412.
5. **Rajeshkumar V, Rengasamy R, Naidu PV and Kumar A** (2019) A compact meta-atom loaded asymmetric coplanar strip-fed monopole antenna for multiband operation. *AEU – International Journal of Electronics and Communications* **98**, 241–247.
6. **Reddy VV and Sarma NVSN** (2014) Compact circularly polarized asymmetrical fractal boundary microstrip antenna for wireless applications. *IEEE Antennas and Wireless Propagation Letters* **13**, 118–121.
7. **Ganesan I, Kavitha K and Paulkani I** (2018) Self complementary frequency independent triple band sinuous antenna array for wireless applications. *Progress In Electromagnetics Research Letters* **78**, 89–95.
8. **Kumar A, Saravanakumar M and Raghavan S** (2018) Dual-frequency SIW-based cavity-backed antenna. *AEU – International Journal of Electronics and Communications* **97**, 195–201.
9. **Sivasundarapandian S and Suriyakala C** (2017) A planar multiband Koch snowflake fractal antenna for cognitive radio. *International Journal of Microwave and Wireless Technologies* **9**, 335–339.
10. **Hwang KC** (2007) A modified Sierpinski fractal antenna for multiband application. *IEEE Antennas and Wireless Propagation Letters* **6**, 357–360.
11. **Malik J, Kalaria P and Kartikeyan M** (2013) Complementary Sierpinski gasket fractal antenna for dual-band WiMAX/WLAN (3.5/5.8 GHz) applications. *International Journal of Microwave and Wireless Technologies* **5**, 499–505.
12. **He Y, Li L, Zhai H, Dang X, Liang C-H and Liu Q-H** (2010) Sierpinski space-filling curves and their application in high-speed circuits for ultra-wideband SSN suppression. *IEEE Antennas and Wireless Propagation Letters* **9**, 568–571.
13. **Elavarasi C and Shanmuganantham T** (2017) SRR Loaded periwinkle flower shaped fractal antenna for multiband applications. *Microwave and Optical Technology Letters* **59**, 2518–2525.
14. **Gupta A, Joshi H and Khanna R** (2017) An X-shaped fractal antenna with DGS for multiband applications. *International Journal of Microwave and Wireless Technologies* **9**, 1075–1083.
15. **Mishra GP and Mangaraj BB** (2019) Miniaturised microstrip patch design based on highly capacitive defected ground structure with fractal

https://doi.org/10.1017/S1759078720000343 Published online by Cambridge University Press

boundary for X-band microwave communications. *IET Microwaves, Antennas & Propagation* **13**, 1593–1601.
16. **Behera S and Vinoy KJ** (2012) Multi-port network approach for the analysis of dual band fractal microstrip antennas. *IEEE Transactions on Antennas and Propagation* **60**, 5100–5106.
17. **Hwang KC, Kim HB and Nguyen Thi T** (2013) Dual-band circularly polarised Spidron fractal microstrip patch antenna for Ku-band satellite communication applications. *Electronics Letters* **49**, 444–445.
18. **Mopidevi H, Rodrigo D, Kaynar O, Jofre L and Cetiner BA** (2011): compact and broadband antenna for LTE and public safety applications. *IEEE Antennas and Wireless Propagation Letters* **10**, 1224–1227.
19. **Mopidevi H, Damgaci Y, Rodrigo D, Jofre L and Cetiner BA** (2014) A quad-band antenna for public safety applications. *IEEE Antennas and Wireless Propagation Letters* **13**, 1231–1234.
20. **Lizzi L, Azaro R, Oliveri G and Massa A** (2016) Multiband fractal antenna for wireless communication systems for emergency management. *Journal of Electromagnetic Waves and Applications* **26**, 1–11.
21. **Singh G and Singh AP** (2018) On the design of planar antenna using Fibonacci word fractal geometry in support of public safety. *International Journal of RF and Microwave Computer-Aided Engineering* **29**, e21554. https://doi.org/10.1002/mmce.21554.
22. **Kakkar S, Kamal TS and Singh AP** (2019) On the design and analysis of I-shaped fractal antenna for emergency management. *IETE Journal of Research* **65**, 104–113.
23. **Sagan H** (1994) *Space-Filling Curves*. New York: Springer.

Paulkani Iyampalam received her B.E degree in Electronics and Communication Engineering from Kings Engineering College, Chennai, India and M.E degree in Communication Systems from Mepco Schlenk Engineering College, Sivakasi, Tamil Nadu, India. Now, she is working towards her Ph.D. at Mepco Schlenk Engineering College, Sivakasi, Tamil Nadu, India. She is an associate member of the Institution of Engineers (India). Her research interest includes metasurface antennas, smart antennas and fractal antennas.

Indumathi Ganesan has 21 years of experience in teaching and research at Mepco Schlenk Engineering College, India. She received her B.E degree in Electronics and Communication Engineering and M.E degree in communication systems from Madurai Kamaraj University, Madurai, India. She completed her Doctoral program in the field of Wireless Communication from Anna University, Chennai, India. She is working as a professor in the Department of Electronics and Communication Engineering in Mepco Schlenk Engineering College, Sivakasi, Tamil Nadu, India. She is a lifetime member of ISTE, IEI and FIETE. Her main research interests are wireless communication, digital signal processing and antenna design. She has published 90 research papers in various international, national journals, and conferences.

https://doi.org/10.1017/S1759078720000343 Published online by Cambridge University Press